Structure and dynamics of water in tendon from NMR relaxation measurements

Stéphane Peto, Pierre Gillis, and Victor P. Henri
Physique Expérimentale, Groupe de Résonance Magnétique Nucléaire, Faculté de Médecine, Université de Mons-Hainaut, B 7000 Mons, Belgium

ABSTRACT Nuclear magnetic relaxation times were measured in collagen tissue when varying the orientation of the fiber with respect to the static field. T_1 was found to be only slightly dependent on θ, the fiber-to-field angle, but T_2 was very sensitive to the orientation, with a maximum value at the magic angle. The transverse decay curves were multiexponential. Their deconvolution displayed four components; the ones that decayed most slowly were almost independent of θ, but the two fastest ones showed a strong angular dependence that was interpreted with a cross-relaxation model. Quadrupolar dips were visible in the $1/T_1$ dispersion curves. These dips were independent of θ, so that the magnetization transfer could also be assumed to be independent of the fiber orientation. Finally, each component was assigned to a fraction of protons localized in the macromolecular structure and characterized by particular dynamics. The model of Woessner was applied to the water molecules tightly bound into the macromolecules, which resulted in a dynamical description of this water fraction. This description is compatible with the two-sites model of Ramachandran based on x-ray diffraction and with the extensive studies of Berendsen. However, the important indications obtained from the deconvolution lead to a less static representation of the tissue.

INTRODUCTION

Longitudinal (T_1) and transverse (T_2) relaxation times of water protons are shorter when measured in biological tissues than when measured in pure water. The ratio of T_1/T_2 in the tissues is also somewhat larger than in pure water. The relaxation rates, moreover, depend on the strengths of the magnetic fields (1) in the usual frequency range (between 0.01 and 100 MHz).

An explanation of these facts was originally provided by a simple model in which it was assumed that two different water fractions are present, each characterized by its own dynamics. They are referred to as the "bound" (i.e., influenced by the macromolecules) and the "free" fractions (2, 3). Within this model, and with the additional assumption of fast exchange between the water from the two fractions (4), it was possible, for instance, to explain the fact that the observed single rate $1/T_1$ is a weighted mean of the relaxation rates inside each fraction in the absence of exchange.

However, an analysis of the transverse relaxation decay curves, obtained from measurements in rat muscles, suggested to Hazlewood et al. (5) that there must be at least three different water fractions. Using the Zimmerman–Brittin model (6), they analyzed the data using three exchange rates and showed that these three fractions appear to exchange water molecules slowly among themselves, but that each fraction might also contain fast-exchanging subfractions. Resing (7, 8) did a theoretical analysis of the cases where fast-exchange conditions do not apply and emphasized the importance of an "intermediate" exchange rate.

Proton exchange between sites separated by a chemical shift is an important process in aqueous, heterogeneous systems (9) and has been extensively studied by Gutowsky and co-workers (10–12). Fung (13, 14) suggested that the nonexponential decay of spin echo in muscle water is mainly due to hydrogen exchange between water and functional groups in the proteins. It is thus generally agreed that in muscle tissues the magnetization goes through the different proton compartments by exchanging entire water molecules or hydrogen atoms.

These chemical exchange models neglect cross-correlation, the effect of magnetic coupling between fractions, ie., the relaxation resulting from a magnetization transfer at the interface. The fraction with the shortest proton relaxation time acts as a relaxation sink for the other fraction (15). Escanye (16) has investigated the longitudinal relaxation in frozen mouse tissue and has isolated nonfreezable water, which was identified as water bound to macromolecules. This study leads one to consider the dominating contribution of intermolecular dipolar interaction and of cross-relaxation between the water and protein protons. Several experimental procedures for the display of cross-relaxation are described by Edzes and Samulski (17, 17*a*), Fung and McGaughy (18), Renou et

0006-3495/90/01/71/14 $2.00

al. (19), and Wise and Pfeffer (20). They were successfully applied in the case of collagen fibers and muscle tissues.

We present here our results on water proton relaxation time measurements in collagen fibers. This biological material is of interest because of the high anisotropy of its macromolecular arrangement, which allows the introduction of an additional parameter: the fiber orientation with respect to the static field H_0. The effect of the collagen fiber orientation on the dipolar splitting of the spectra has been known for some time (21–25); Berendsen has shown that the separation between the resonance peaks depends on the angular factor $(1-3\cos^2\theta)$, where θ is the angle between the fiber axis and the direction of the static magnetic field. Cleveland et al. (26) have determined the angular dependence of the spin diffusion coefficient for water protons in muscles: the variation of this coefficient is of the order of 25-30% when moving the sample from a position aligned with H_0 to a position orthogonal to H_0. Kasturi et al. (27) have also observed an anisotropy effect of ~5% on the transverse relaxation time T_2 with no significant effect on T_1. Our experiments on collagen fibers confirm these observations and also add to them. The transverse relaxation time is much more sensitive than the longitudinal time to the orientation of the fiber, and the "magic angle" of 55° is clearly a particular orientation corresponding to a maximum for T_2. The transverse decay curves for collagen are multiexponential and our data require, for their description, four single exponential functions, whereas previous data on collagen published by Fullerton et al. only required two exponentials (28).

Assuming the existence of four water fractions and applying the exchange model to the two components with the largest angular dependence (the two most rapidly decreasing components), and without making any assumption on the exchange mechanism, we have determined the intrinsic parameters of the system: relaxation times, population fractions, and characteristic exchange times. The observed temperature dependence of the exchange rate is explained in the two fastest components by the dominance of the cross-relaxation between macromolecular and bound water protons. In this case, the expression of the exchange times characteristic of the magnetization transfer can be derived from spectral density functions, for which some authors suggested the use of Lorentzians (29, 30); this last assumption is not needed in our study. To examine the magnetization transfer mechanisms, we present measurements of the quadrupolar dips appearing in the $1/T_1$ dispersion curves of collagen fibers (31–33); these dips are shown to be independent of the orientation of the fiber in H_0 and thus, only the intrinsic relaxation times depend on the orientation.

Finally, from the previously reported localization of the water molecules in the macromolecular structure (34–38), we have associated the observed populations with the fractions assumed in our model, and we have, with reasonable dynamical assumptions, been able to explain the T_2 enhancement at the magic angle.

EXPERIMENTAL PROCEDURE

Sample

Samples of collagen fibers were extracted from pig legs. Tissues were rapidly excised and immediately placed in NMR tubes. Samples of 0.15 and 0.3 g were used, with a water content of ~60% in weight. Collagen, being an inert tissue (poor in cells), is very stable over time. Therefore, measurements performed with it give very reproducible results.

NMR measurements

Relaxation times were measured at the proton Larmor frequency of 20 MHz on a pulsed spectrometer (model PC 20; Bruker Instruments, Billerica, MA). Static field was achieved with a 0.47-T magnet and was perpendicular to the NMR tube axis. A single coil was used for radiofrequency pulse emission and FID detection. The temperature of the sample ranged from 10°C to 30°C (± 1°C) thanks to freon liquid (CF4) regulation.

T_1 was measured using the inversion–recovery sequence $180° - \tau - 90°$; 12 points were collected. The delays τ were logarithmically distributed, following $\tau_j = c_j T_1$, with $c_j = 0.04 \times 128^{(j-1)/(n-1)}$, where T_1 is an approximate value of the relaxation time and n is the number of points ($j = 1, n$). The FID was sampled 200 μs after the 90° pulse and each point was measured four times.

T_2 measurements were performed using the CPMG sequence $90° - \tau - (180° - 2\tau)n$, with τ = 100, 150, 500, and 1,000 μs, and where n is the number of 180° pulses between two consecutive amplitude acquisitions. Every echo decay was obtained from several scans of 165 points each, all scans being repeated 400 times to increase the accuracy. For τ = 100 μs, three scans were recorded: the first echo was followed by an n = 1 sequence, an n = 6 sequence, and an n = 10 sequence. For τ = 150 μs, three scans were also recorded (the first echo plus n = 2, n = 4, n = 7); for τ = 500 μs, two scans (the odd and the even numbered echoes, respectively) were taken and only one (n = 1) for τ = 1,000 μs. The echo decay curves obtained in this way range from the first echo to t = 330 ms.

For the T_2 measurements, the spectrometer was connected to a personal computer which stored the data. The data were then transferred from the PC to an IBM 4341 computer. We first analyzed the data by using a simple graphical method in order to isolate the different components of the multiexponential transverse decay curves. The method consists of separating the components by linear regression on a semi-logarithmic plot. The results of this preliminary analysis were then introduced as initial values in a computer program, "Minuit," based on the Simplex method which proceeds by χ^2 minimization. The program provides, after convergence, the value of each parameter of the theoretical function (the amplitude and decay rate of each exponential) with the corresponding χ^2 and covariance matrix.

The $1/T_1$ dispersion curves were recorded on a field cycling system (relaxometer) developed at the IBM T.J. Watson Research Center (Yorktown Heights, NY) (1). This system allows measurement of T_1 at frequencies ranging from 0.01 to 50 MHz.

RESULTS

T_1 measurements

Results of the T_1 measurements at 37°C for the aligned ($\theta = 0°$ and $\theta = 180°$) and orthogonal ($\theta = 90°$ and $\theta = 270°$) orientations of the collagen fiber with respect to H_0 are shown on Fig. 1. 60 measurements were performed for each orientation. The assumption that the distributions of the T_1 values are Gaussian is acceptable because p, the probability of being wrong if rejecting this hypothesis, is 0.2. The average values of T_1 are, respectively, 200 and 204 ms for the two orientations, with a standard deviation of $\sigma = 6$ ms. From this, it can be seen that within the errors ($3\sigma = 18$ ms), it is at first consideration impossible to claim any significant difference in T_1 for the two orientations. Nevertheless, statistical tests show that the average values of T_1 for any combination of two nonequivalent orientations are different ($p < 0.01$), whereas for the two aligned ($p = 0.6$) or the two orthogonal positions ($p = 0.7$) the average T_1 is equal. From this it may be concluded that a slight anisotropy effect (2%) occurs for the longitudinal relaxation time at 20 MHz.

The $1/T_1$ dispersion curves (Fig. 2) represent the value of $1/T_1$ as a function of the proton Larmor frequency. The dispersion curves are quite similar for $\theta = 0°$, 55°, and 90° (not shown). A difference of 2% at 20 MHz is clearly below the accuracy of the relaxometer for the conditions of our measurements. Nevertheless, this study shows that the longitudinal magnetization decays are better adjusted with two exponential functions than with only one. The difference is slight but reduces the error of the fit by a factor of two or three (Fig. 3).

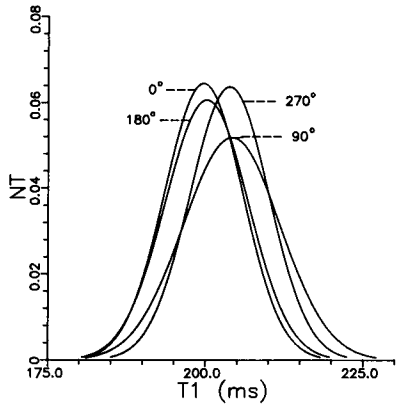

FIGURE 1. The histograms of the 60 measurements of T_1 have a Gaussian distribution for each orientation. The curves present the Gaussian probability densities of the T_1 measurements for the four orientations of the fiber with respect to the static field H_0 at 37°C: 0° and 180° when the fiber axis is aligned along the H_0 direction, and 90° and 270° for the orthogonal positions.

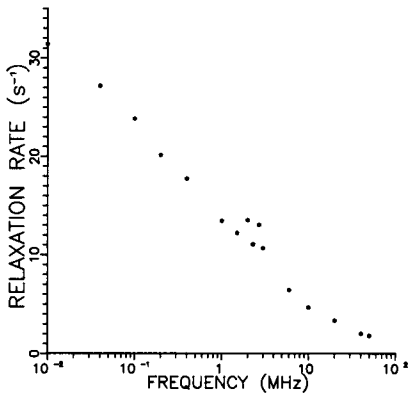

FIGURE 2. $1/T_1$ dispersion curve at 37°C of a collagen sample with the fiber axis orthogonal to the static magnetic field. Notice the peaks between 1 and 4 MHz.

T_2 measurements

Fig. 4 shows the decay curves for the 0° and 55° orientations of the collagen fiber with respect to the static magnetic field. The anisotropy effect is evident and the curves are multiexponential. Figs. 5, *a* and *b*, where the results are treated as single exponentials, are particularly instructive. The amplitude and relaxation time of the single exponential fit are plotted versus the angle θ of the sample with respect to the static field. Note in Fig. 5, *a* and *b*, that the curves are characterized by four maxima at the positions $\theta = 55°$, 125°, 235°, and 305°. These angles all correspond to an angle of 55° (the "magic angle") between the sample axis and the magnetic field direction. We are thus led to examine the relaxation for the angles 0°, 55°, and 90°. Our measurements show that the amplitude of the first sampled echo (200 μs) does not depend on the orientation. This independence may reasonably be extrapolated to the initial conditions, so that the angular dependence of the amplitude shown in Fig. 5 *a* has to be understood as a global effect of the monoexponential fit (known to be incorrect), rather than as real information about initial conditions. Moreover, the end of the decay is independent of the fiber-to-field angle. These results are in good agreement with the previously reported study of Berendsen (21), who plotted the inverse peak-to-peak amplitudes of the derivative of the resonance curves in collagen spectra against the orientation of the sample. Fullerton et al. (28) reported for collagen the dependence of the spin-echo amplitude of the short relaxation time component (calculated from a two-component deconvolution) versus the angle θ. However, the orientation behavior of the long time component is quite different. This might be due to the fact that the long component is not perfectly isolated and that it contains

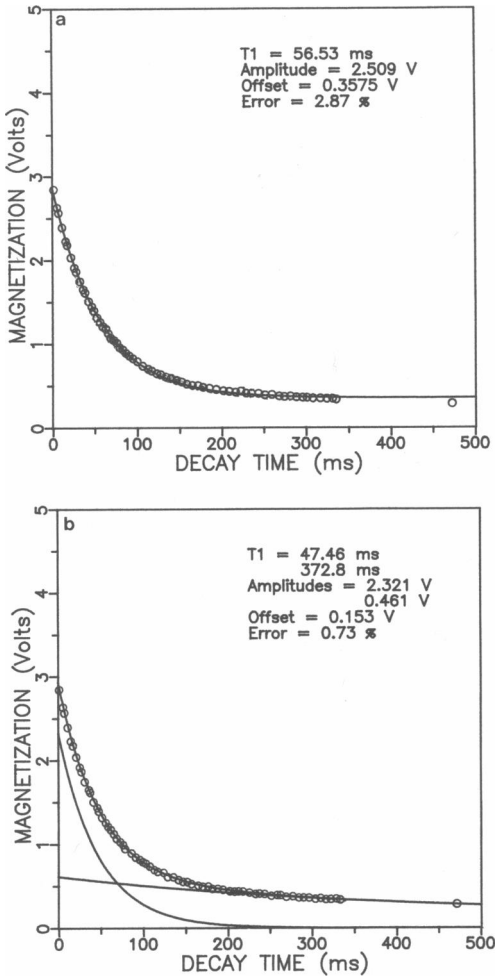

FIGURE 3. Decay of the longitudinal magnetization (0.1 MHz, 37°C), fitted, respectively, with a single exponential (*a*) and with two exponential functions (*b*). The relaxation times (T_1) and the amplitudes of the fits are indicated on the graph with the corresponding errors. The improvement due to the second exponential is especially visible on the last point, corresponding to the equilibrium magnetization, which was measured eight times to compensate for the low value of the signal.

the influence of the shortest components, which depend strongly on the orientation; the 31 data points were actually correctly fitted by a sum of two exponential functions, but the curves must be interpreted as due to the average of a more complex transverse decay.

T_2 obtained from CPMG sequences are generally dependent on the pulse repetition rate. This dependence may be attributed to several causes that are discussed below. Fig. 6 shows the transverse decay curves for 0° and 55° orientations of the fiber at 20°C for four values of τ (100, 150, 500, 1,000 μs built with, respectively, 496, 496, 331, and 165 sampled echoes). The results for the three largest values of τ are very similar, the only observable difference appearing between 100 and 150 μs.

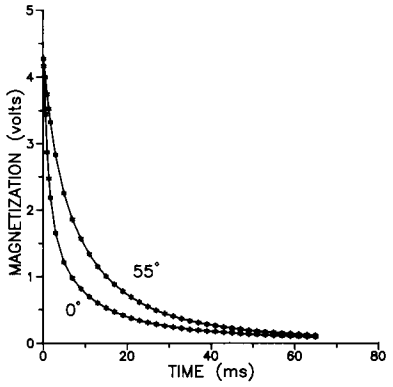

FIGURE 4. Transverse decay curves at 30°C for fiber-to-field angles of 0° and 55°. The 496 collected points are not all represented and the solid line simply connects the points.

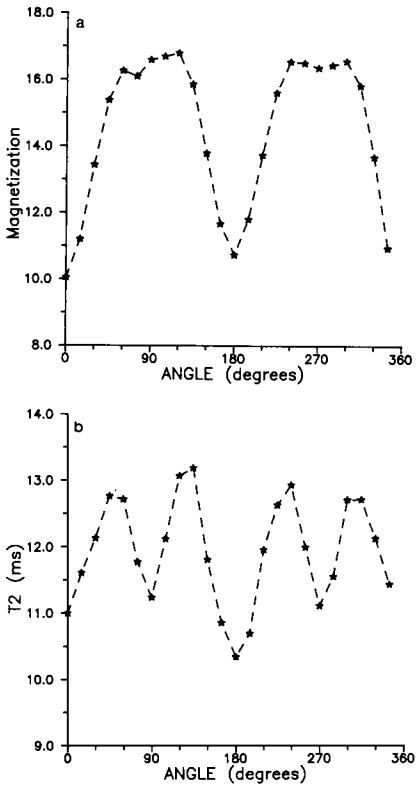

FIGURE 5. Single exponential fit of the transverse decay: initial amplitude (*a*) and transverse relaxation time (*b*) versus the orientation of the collagen fiber with respect to the magnetic static field. Fitting the curves with a single exponential displays the global average dependence of the transverse decays on the fiber-to-field angle; the maxima correspond to angles separated by 55° from the position aligned to the static field.

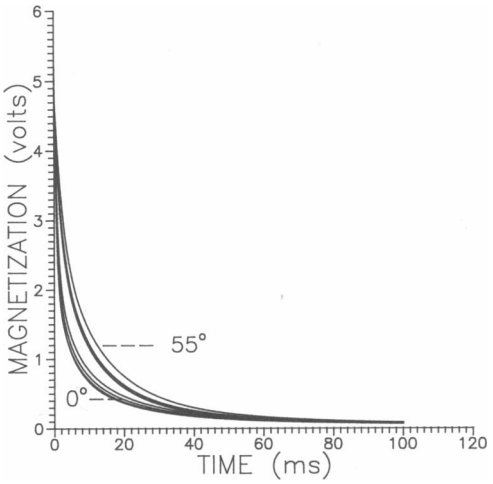

FIGURE 6. Decay of the transverse magnetization at 20°C for two fiber-to-field angles (0° and 55°) using different values of the interpulse delay τ (100, 150, 500, and 1,000 μs) in a CPMG pulse sequence. These curves are the adjustments of the experimental data performed with the parameters of Table 1. For both orientations, the most important variation occurs between τ = 100 μs and τ = 150 μs: the relaxation rate increases for increasing delay τ.

Experimental data were adjusted with four exponentials and a constant that takes electronic offset and background signal into account (Table 1). For τ = 100 μs, the nine parameters of the fit can be determined in a straightforward manner, the total amplitude being the same for both orientations. When increasing τ from 150 to 500 μs, the loss of short time information is drastic, and the total amplitude has to be fixed from the results obtained with τ = 100 μs in order to determine univocally the fastest component, especially when θ = 0°. The τ = 1,000 μs results are well fitted by a three-component decay, and a fourth one, the fastest, may or may not be added arbitrarily.

The observed difference between τ = 100 μs and τ = 150 μs only affects the fastest component. It would have been consistent with our interpretation of the τ dependence to achieve the deconvolution of T_2 results from the measurements with τ = 150 μs, because we think that the relaxation time measured with a pulse repetition time of 100 μs is slightly influenced by a spin-locking effect. However, the variation between τ = 100 μs and τ = 150 μs is tenuous, and information about the fastest relaxation is imprecise when extracted from the τ = 150 μs results. Moreover, we are mainly interested in the orientation dependence of T_2, which is much more important than the difference between τ = 100 μs and τ = 150 μs results. Another reason that compelled us to analyze the decay with τ = 100 μs is that the first sampled echo was measured to be the same for different orientations while for the other values of τ, the amplitude of the first sampled echo vary with the fiber-to-field angle.

The deconvolution of the decay curves provides information about the change of the amplitude and of the relaxation time when modifying the position of the fiber in the field H_0. Table 2 shows the results of three fiber-to-field angles (θ = 0°, 55°, and 90°) at three temperatures (10°C, 20°C, and 30°C) and presents the nine parameters of the adjustment with four exponential functions and with a constant. The computer program (Minuit) defines the error in terms of an error covariance matrix corresponding to the nine parameters of the function. The diagonal elements of the error matrix are the squares of the individual errors on the parameters, including the effect of correlation with the other parameters. The minimization problem is usually straightforward (convergence), but the calculation or interpretation of the resulting parameter uncertainties is considerably more

TABLE 1 Parameters of the fit of the decay of the transverse magnetization by the function $F(t) = \Sigma_{i=1}^{4} M_{oi}\, e^{-t/T_{2i}} + C$

Delay τ	Orientation	A_1	T_{21}	A_2	T_{22}	A_3	T_{23}	A_4	T_{24}	C
μs			ms		ms		ms		ms	
100	0°	0.55	0.85	0.23	4.8	0.18	16.3	0.04	67	0.006
	55°	0.37	1.8	0.36	8.2	0.23	20	0.03	74	0.007
150	0°	0.57	0.78	0.21	4.2	0.18	15	0.04	67	0.007
	55°	0.38	1.6	0.34	6.8	0.24	18.3	0.03	85	0.006
500	0°	0.60	0.67	0.21	4.7	0.15	14.5	0.03	68	0.006
	55°	0.40	1.6	0.35	7.2	0.21	18.4	0.03	83	0.006
1,000	0°	0.62	0.65	0.18	4.5	0.16	15.3	0.03	73	0.005
	55°	0.43	1.6	0.34	7.6	0.20	19.1	0.03	83	0.005

M_{oi} is the normalized amplitude of the exponential function i and T_{2i} is the corresponding observed transverse relaxation time. C is a constant for the offset. The nine parameters are given for two orientations of the fiber with respect to the static field (0° and 55°) and for different values of the interpulse delay τ in the CPMG sequence: τ = 100, 150, 500, and 1,000 μs. As explained in the text, for τ = 1,000 μs the fastest component is arbitrary; we have added the component that arises from the 500 μs data for the sake of comparison.

TABLE 2 **Parameters arising from same fit as in Table 1, but corresponding to transverse decay measurements performed for three orientations of fiber in H_0 (0, 55, 90°) at three temperatures (10, 20, 30°C), with 100-μs pulse delay.**

Temperature	Orientation	M_{01}	T_{21}	M_{02}	T_{22}	M_{03}	T_{23}	M_{04}	T_{24}	C
			ms		*ms*		*ms*		*ms*	
10°C	0°	0.53	0.5	0.26	3.4	0.17	17.3	0.04	66.9	0.003
	55°	0.33	1.8	0.34	7.8	0.29	22.5	0.04	87.2	0.003
	90°	0.40	1.6	0.33	6.3	0.23	20.9	0.03	80.4	0.003
20°C	0°	0.57	0.7	0.23	4.4	0.16	16.9	0.03	67.5	0.004
	55°	0.39	2.8	0.40	10.6	0.18	25.5	0.03	89.7	0.004
	90°	0.48	2.4	0.35	9.3	0.15	24.7	0.02	90.5	0.005
30°C	0°	0.56	1.1	0.26	6.0	0.15	18.9	0.03	79.8	0.005
	55°	0.42	3.8	0.41	12.8	0.13	20.7	0.04	79.1	0.004
	90°	0.50	3.5	0.38	11.8	0.09	24.2	0.03	88.8	0.005

complicated and must be considered very carefully. The quality of the fit has been tested by calculating the average of the relative differences between theoretical and experimental values: for Tables 1 and 2, the mean difference is always <2%. Moreover, two independent checks were performed: the first consists of subtracting three components from the total curve (the difference must be monoexponential) and the second consists of adding a fifth component, which should not improve the fit.

The existence of four components indicates the presence of at least four proton populations characterized by intrinsic relaxation times clearly different from each other. The normalized amplitudes and the relaxation times of the two fastest components depend strongly on the orientation. Their decay rates are minimum at the magic angle. Because of previous demonstrations of the existence of cross-relaxation in collagen (17–20), these two components are likely to arise from the macromolecular protons for the fastest decaying one and from the tightly bound water protons for the other one.

Quadrupolar dips

Peaks are observed in the $1/T_1$ dispersion curves of some biological systems such as collagen, in a region between 1 and 4 MHz. These frequencies correspond to the resonance between the Zeeman energy for the protons and the quadrupolar splitting of the ^{14}N nuclei in the protein N—H groups. The cross-relaxation between the nuclei is maximum when the difference between the proton Zeeman levels coincides with the ^{14}N energy level splitting. At these energy level crossings, the N—H protons become relaxation sinks for protons of water molecules bonded to macromolecules (33). The water magnetization is thus eliminated in two steps: the N—H protons absorb magnetization from the water molecules' protons and these N—H protons transfer their energy to the N nuclei. This phenomenon explains the relaxation rate enhancement at the peaks. Governed by the same mechanisms, this relaxation process allows study of cross-relaxation at the water–macromolecule interface, even for frequencies far from the frequencies of the peaks. In particular, it is possible to verify whether the quadrupolar dips are modified when moving the orientation of the fiber in H_0.

Fig. 2 shows a complete dispersion curve at 37°C; it is identical for the three fiber orientations at 0°, 55°, and 90°. Fig. 7 shows the details of the peaks for the three positions; within the errors (1–2%), the peak structure does not show any significant differences.

This study confirms the importance of cross-relaxation occurring between water protons and macromolecular protons, and indicates that the rate of magnetization transfer is independent of the sample orientation.

DISCUSSION

T_1 and T_2 behave very differently in the conventional frequency range (above 0.01 MHz for the proton resonance frequency), at least when one looks at the effects of anisotropy and multiexponentiality.

The standard expression for the relaxation times by spectral densities indicates that $1/T_1$ is only sensitive to correlation times shorter than the Larmor period, whereas all correlation times contribute to $1/T_2$. Consequently, the bound water fraction influenced by the macromolecules (for instance, by the tumbling of the macromolecules, or because the macromolecules confine water motion) is characterized by an anisotropic dynamics too slow to participate in longitudinal relaxation. Moreover, the anisotropic reorientation of the magnetic dipolar interaction induces a supplementary dephasing of the spins which considerably shortens T_2.

T_2 is thus shorter than T_1, and the exchange times between fractions must be compared with the relaxation times. Compared with T_1, these exchange times are short, resulting in a fast exchange behavior. In the case of T_2,

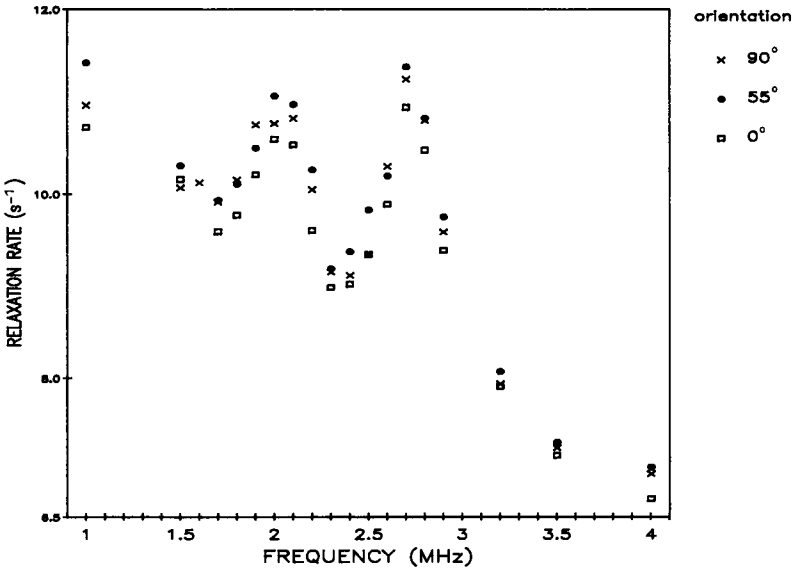

FIGURE 7. The details of the quadrupolar dips appearing in the dispersion profiles of Fig. 2, for three fiber-to-field angles (0°, 55°, and 90°).

the exchange times are long enough to lead to a multiexponential decay.

The results of Table 2 clearly show that the fastest components' relaxation is orientation dependent, whereas the relaxation of the slowest components essentially is not. That feature has led us to introduce a decoupling between the evolutions of the two groups of components, and to concentrate our analysis exclusively on the fast components. Indeed, it is quite reasonable to assume that the times characterizing the exchange between the decoupled modes is shorter or equal to the intrinsic relaxation times T_{23} and T_{24}, but long compared with T_{21} and T_{22}. The slight nonexponentiality of the longitudinal relaxation is a supplementary argument of the same sort: the exchange time may not be much shorter than the measured relaxation times that correspond to the slowest relaxing fractions, as explained above.

Pulse spacing dependence

Only the fastest component relaxation depends on the pulse separation in a CPMG sequence (2τ). We successively examine three possible sources for this dependence: (*a*) diffusion through the static field inhomogeneities, (*b*) proton exchange between sites separated by a chemical shift, and (*c*) the shift from a T_2 measurement to a $T_{1\rho}$ measurement when τ becomes very short.

(*a*) The static field inhomogeneity of the Bruker PC 20 has been estimated by comparing the FID and the CPMG T_2 decay of a nondiffusing lipid system. It is of the order of 1 G/cm. We may thus in turn estimate the self-diffusion coefficient that is necessary for explaining a change in $1/T_2$ (1,200 s^{-1} becoming 1,300 s^{-1}) when τ goes from 100 to 150 μs. It is of the order of 12 cm^2/s at 20°C, a quite unreasonable value. We conclude that molecular diffusion is negligible in our measurements. This is confirmed by Fullerton et al. (28), who found that T_2 measured with a Hahn spin–echo sequence is equivalent to T_2 measured with a CPMG pulse sequence.

(*b*) Collagen spectra are characterized by three lines (23): a doublet of outer lines that Berendsen assigns to tightly bound water protons, the splitting being due to intramolecular dipolar coupling, and a central peak, essentially assigned to mobile side chains of the proteins. The assignment made through our deconvolution is parallel to the spectral analysis of Berendsen: the fastest component is associated with mobile macromolecular protons, while the second component (A_2 and T_{22} in Tables 1 and 2) is attributed to tightly bound water protons.[1] The component that depends on τ corresponds to the central line. That line does not appear to split even at low temperature, which would be the case for proton exchange between sites of different energies. We thus also reject this second explanation.

(*c*) When τ, the interpulse delay in a CPMG sequence, is short compared with all the microscopic time constants characterizing the irreversible mechanisms (resonant off-

[1]The relaxation of the second component does not depend on τ. That means that any proton exchange between water molecules must be slower than the pulse repetition rate. Moreover, the agreement between our deconvolution and Berendsen's spectral analysis is reinforced by the fact that the width of the central line and the doublet separation are both orientation dependent, just as T_{21} and T_{22} in Table 2.

set, chemical shift, and spin–spin coupling), the decay of the transverse relaxation does not define any more T_2, but rather $T_{1\rho}$, the relaxation time in the rotating frame given at a spin-locking frequency (39):

$$\nu_1 = 1/4\tau. \tag{1}$$

The spectral dependence of $1/T_{1\rho}$ does not contain any secular term (zeroth order spectral density function). The τ-dependence of the T_2 measurements arises then from the dispersion of $T_{1\rho}$, which is the same as the T_1 dispersion (41). It is well known that T_1 is modified around a given frequency, say ν_0, if motions with a time constant of the order of $1/\nu_0$ occur in the system. If τ_0 is the characteristic time of the slowest motions in the system, there will be no dispersion for frequencies smaller than $1/\tau_0$. Our T_2 measurements show very little variation for $\tau > 150$ μs, i.e., for frequencies <1,666 Hz, thanks to Eq. 1, if we consider $T_{1\rho}$ measurements. A very simple interpretation can therefore be suggested for the τ-dependence of our results: the only observed variation, happening between $\tau = 100$ μs and $\tau = 150$ μs, corresponds to the beginning of T_1 enhancement when H_0 increases, situated about $\nu = 2{,}000$ Hz, arising from the slowest motions in the sample. That interpretation, although not proven, is quite compatible with the T_1 dispersion profile shown in Fig. 2. Moreover, the pulse delay dependence only appears for the fastest component, which is effectively associated with the proton population characterized by the slowest motions: the macromolecular proton population.

Exchange model

As mentioned above, the two fastest decreasing components can reasonably be assigned to protons of functional groups on the macromolecules and to bound water protons. The amplitudes and the relaxation times of these two fractions depend strongly on the orientation, which is not the case for the two other components, with a particular behavior at the 55° position that can be interpreted as follows. The interaction responsible for the relaxation of the protons is the magnetic dipolar interaction; it vanishes when the angle between the static field and the internuclear direction is 55°. In collagen, the vectors joining the bound water protons as well as the macromolecular protons are, on the average, aligned on the fiber axis. Thus, simply assuming that the average proton–proton directions coincide with the fiber direction, a $(1 - 3\cos^2\theta)$ angular dependence for the transverse relaxation rate can easily be explained as being due to magnetic dipolar interaction (see below).

Furthermore, the strong amplitude variations suggest the occurrence of an intermediate regime for the exchange between the two "fastest" fractions. In this range of rates, the observed relaxation times and amplitudes differ from the intrinsic values in each fraction, contrary to what occurs when the exchange is slow. The evolution toward equilibrium of the transverse magnetizations of the fastest fractions is governed by the equations:

$$\begin{aligned}\frac{dM_a}{dt} &= -\frac{M_a(t)}{T_a} - \frac{M_a(t)}{K_a} + \frac{M_b(t)}{K_b}\\ \frac{dM_b}{dt} &= -\frac{M_b(t)}{T_b} - \frac{M_b(t)}{K_b} + \frac{M_a(t)}{K_a},\end{aligned} \tag{2}$$

where M_a and M_b are the magnetization of each fraction, T_a and T_b are the intrinsic relaxation times, and K_a and K_b are the average exchange times in each fraction.

Eq. 2 concerns only the two fastest fractions since it is assumed that the two other fractions exchange much more slowly with the fastest ones, so that their contribution in Eq. 2 is negligible, and the evolutions of the two groups of fractions are decoupled.

The solution of Eq. 2 is the sum of two exponential functions:

$$h(t) = p_\alpha e^{-t/T_\alpha} + p_\beta e^{-t/T_\beta}, \tag{3}$$

where T_α and T_β are the observed relaxation times and p_α and p_β are the normalized coefficients of the two decay modes ($p_\alpha + p_\beta = 1$).

Moreover, the equilibrium balance requires that

$$p_a/K_a = p_b/K_b, \tag{4}$$

where p_a and p_b are the normalized intrinsic population fractions (with $p_a + p_b = 1$).

One can establish in a straightforward manner the relations that give the observed parameters as a function of the characteristics of the model:

$$\begin{aligned}T_\alpha &= f(T_a, T_b, p_a, K_a)\\ T_\beta &= f(T_a, T_b, p_a, K_a)\\ p_\alpha &= f(T_a, T_b, p_a, K_a)\end{aligned} \tag{5}$$

or obtain some of the characteristics of the model (three out of four) as a function of the observed parameters:

$$\begin{aligned}T_a &= f(T_\alpha, T_\beta, p_\alpha, p_a)\\ T_b &= f(T_\alpha, T_\beta, p_\alpha, p_a)\\ K_a &= f(T_\alpha, T_\beta, p_\alpha, p_a).\end{aligned} \tag{6}$$

Our measurements allow the determination of the exchange time K_a. At each temperature, the observed parameters are measured for three experimental conditions (for the three fiber orientations). The intrinsic relaxation times are assumed to vary with the orientation, whereas the population fractions and the exchange times are independent of the angle. T_a, T_b, and K_a are deter-

mined from the four parameters appearing in Eq. 6. T_α, T_β, and p_α are given by the measurements, but p_a is still unknown. Its value is introduced in Eq. 6 as an adjustable parameter, the correct value being the one that renders the three calculated values of K_a equal to each other (for the three different orientations at a given temperature). Table 3 presents the intrinsic parameters and characteristic exchange times. The relaxation times for the fiber-to-field angle of 55° was impossible to determine by our procedure: a slight variation of p_a around its correct value (for which K_a is the same for the three orientations) results in a very large variation for T_a, contrary to the other parameters which are stable with respect to a variation of p_a.

Concerning the angular dependence of the relaxation times, the factor $(1 - 3\cos^2\theta)$ can be introduced by assuming that T_2 depends both on isotropic (T_{2iso}) and anisotropic (T_{2aniso}) terms:

$$\frac{1}{T_2(\theta)} = \frac{1}{T_{2aniso}} + \frac{1}{T_{2iso}} \tag{7}$$

$$= (1 - 3\cos^2\theta)^n \frac{1}{T_2(90°)} + \frac{1}{T_2(55°)}$$

$$\approx (1 - 3\cos^2\theta)^n \frac{1}{T_2(90°)}, \tag{8}$$

since $1/T_2(55°) \ll 1/T_2(90°)$, and with n to be determined. In our results (Table 3), $n = 2$ since we have approximately

$$T_2(0°) \approx T_2(90°)/4. \tag{9}$$

The $(1 - 3\cos^2\theta)^2$ dependence can be recognized in Fig. 5 *a*; this relation is thus reasonably well verified in our measurements when applying the complete exchange model.

TABLE 3 Parameters arising from the exchange model calculations applied to the two fastest components (T_{2i}, M_{oi}, $i = 1, 2$) in Table 2

Temperature	Orientation	T_A	T_B	P_A	K_A	K_B
		ms	*ms*		*ms*	*ms*
10°C	0°	5.5	0.5			
	55°	—	—	0.29	8	19
	90°	19	1.8			
20°C	0°	7.3	0.8			
	55°	—	—	0.26	10	28
	90°	34.5	2.7			
30°C	0°	9.8	1.1			
	55°	—	—	0.25	14	40
	90°	44	3.9			

Notations $i = 1, 2$ in Table 2 correspond, respectively, to indices B, A in Table 3, and $p_B = 1 - p_A$.

Cross-relaxation

Note that the exchange time increases with temperature. This is additional proof that the coupling between the fractions occurs by spin diffusion, and not by exchange of particles. The magnetization exchange rate is given by spectral density functions that are proportional to correlation times; thus, the exchange time obtained from this rate is effectively an increasing function of temperature, contrary to what is expected for the residence time of the protons.

In this model, the magnetic dipolar coupling dominates the relaxation processes. The two proton fractions consist of macromolecular and bound water protons, and their magnetization decay is coupled by magnetization transfer, and described by Eq. 2.

The relaxation rate of a spin a is the sum of three contributions due respectively, to its intramolecular partner, to water protons belonging to another water molecule, and to the macromolecular protons. Only this last group is responsible for cross-relaxation, and relaxation theory leads to

$$1/K_a = N_b\alpha^2 [1/8\, J^{(0)}_{WM}(0) + 9/8\, J^{(1)}_{WM}(\omega)], \tag{10}$$

where $\alpha^2 = \mu_0\gamma\,\hbar/4\pi$, γ being the proton gyromagnetic ratio, where N_b is the number of protons in the macromolecular fraction, W refers to water protons, and M to macromolecular protons.

The usual profiles of $1/T_1$ dispersion curves for various protein solutions, tissues (1), and heterogeneous systems (40) are compatible with several different analytical forms for $J_{WM}(\omega)$, according to the model describing the system. However, these functions are all characterized by a common low frequency limit, which is proportional to a simple correlation time. This feature is obvious when the adopted spectral density is a Lorentzian, an assumption made by several authors (29, 30), but unnecessary here. Indeed, that feature expresses the actual meaning of a correlation time, i.e., the time beyond which the system forgets its initial conditions, resulting in the vanishing of the correlation function that is associated with it. It may then be written (as a definition)

$$\tau_{CR} \cdot G(0) = \int_0^\infty G(t)\,dt = \frac{1}{2}J(0), \tag{11}$$

so that $J(0)$ is proportional to τ_{CR}, whatever may be the origin of the magnetic dipolar fluctuations, or the physical and chemical processes responsible for the magnetic energy transfer.

It is thus clear that in the extreme narrowing condition ($\omega\tau_{CR} \ll 1$), K_a is proportional to τ_{CR}, but this is also the case when $\omega\tau_{CR} \gg 1$, because of the presence of the zero frequency term in Eq. 10, which then becomes dominant. For both conditions K_a is thus an increasing function of

temperature via the correlation time τ_{CR}. τ_{CR} is the time characterizing the random fluctuations caused by thermal tumbling, which induces mutual spin-flips at the water–macromolecule interface. These characteristic times generally obey

$$\tau_{CR} = \tau_0 e^{\Delta H/kT}, \quad (12)$$

giving the expected temperature dependence. τ_0 is the correlation time at infinite temperature and ΔH is the activation enthalpy of the fluctuation. Usually K_a is considered a parameter governing the magnetization exchange between two fractions in thermal contact (15). The kinetics of this process is then determined by the magnetization difference initially created or maintained by the relaxation times difference. This approach ignores the details of the microdynamics of the cross-relaxation mechanism in favor of a macroscopic description.

Fraction localization

The protein unit that polymerizes to form collagen microfibrils is the elongated molecule called tropocollagen; it is 280 nm long and 1.5 nm wide. Tropocollagen consists of three polypeptide chains intertwined in a triple helix. Collagen fibrils are organized in a parallel arrangement of microfibrils. The fibrils are axially packed, forming fibers that are grouped in bundles constituting the tendon. The fibers are embedded in a matrix, the amorphous ground substance, having the properties of a viscous solution of proteins. The tendon is a tissue poor in cells and its metabolism is extremely reduced; its role is exclusively mechanical. It has been established that the fastest component of our T_2 curves arises from the tropocollagen protons. Water molecules tightly bound to the macromolecular structure constitute a population of protons; these bound water molecules penetrate the triple-helix interstices and are fixed by two hydrogen bonds (interstitial water). The second water fraction is weakly bound and much more mobile but feels the influence of macromolecules; this fraction localized in the fibrils is the hydration water of the tropocollagen. The last fraction fills the space between the fibrils and between the fibers; it is essentially the ground substance. This separation into fractions seems reasonable because the anisotropy only concerns the two fastest decaying components. Certainly the water compartmentation is not perfect and the transition between the compartments is not abrupt, but the experimental results indicate that the interstitial water is relatively isolated from the rest. The limit of the fibrils probably constitutes a very efficient boundary, only weakly permeable to exchanges.

Molecular dynamics

For free and hydration water, the relaxation is comparable to the relaxation of a protein solution that has been extensively studied by Koenig and Brown (1). As in pure water, the relaxation mechanisms combine intramolecular and intermolecular contributions, but the macromolecular tumbling additionally imposes a coherent motion on the water that modifies the conditions of the intermolecular relaxation. Moreover, relaxation of the hydration water is determined by a motional perturbation caused by the presence of the interstitial water on the rigid tropocollagen: in addition to a weak interaction with macromolecules, the accessible space on the macromolecule is reduced by the existence of sites occupied by strongly bound water molecules. This explains why the free and hydration water relaxation times are distinguishable.

The intrinsic relaxation of the protons from the functional groups in tropocollagen occurs by magnetic dipolar interaction among the protons from adjacent groups of the same molecular chain; one proton preferentially interacts with its direct neighbors just below and above it on the chain. The direction of the vector joining these neighboring protons is not parallel to the fiber, at least instantaneously, but because of the rotational motion of the functional groups around their binding point, this direction may be substituted by a mean direction parallel to the fiber. Furthermore, collagen chains are extremely rich in glycine residues (one out of every three). Glycines are the only amino acids small enough to occupy the crowded interior of the collagen triple helix and to form the spine of the macromolecule. Since these entities are unable to move, the interaction among the glycine protons is structurally directed along the fiber axis. It is possible that because this group of protons has difficulty moving their NMR signal is too short to be detectable in our measurements; the particularly long T_2 (T_A in Table 3) for macromolecular protons then means that the calculated T_2 characterizes a signal arising from functional groups that maintain a high mobility. This assumption is consistent with the values of correlation times introduced for the dynamics description.

In the high field approximation, the dipolar interaction can be considered as a weak perturbation and only the $m = 0$ terms subsist in the Hamiltonian (41–43):

$$H'_D = \sum_j \frac{(1 - 3\cos^2\theta_{aj})}{r_{aj}^3}\left[I_a^z I_j^z - \frac{1}{4}(I_a^+ I_j^- - I_a^- I_j^+)\right], \quad (13)$$

where θ_{aj} is the angle between the internuclear vector and the H_0 direction.

For the present macromolecular structure, $(1 - 3\cos^2\theta)$ is factorized out of the sum over j; here θ is the

angle between the average interaction direction and the static field H_0, which is equivalent to the fiber-to-field angle. Therefore, when computing the spectral densities, a $(1 - 3\cos^2\theta)^2$ angular dependence appears for the intrinsic transverse relaxation rate of macromolecular protons. This simple procedure is made possible by the relative immobility of the protons.

The mechanism of magnetization transfer between macromolecular and water protons is a magnetic dipolar contact which is obviously angular dependent. However, this angular dependence concerns each spin–spin interaction, and the geometrical complexity of the water imbrication in the triple helix of the tropocollagen makes it disappear by averaging all spins in the fraction so that the cross-relaxation rate (which concerns the spin diffusion from fraction to fraction) may essentially be considered orientation independent.

For the interstitial water, Ramachandran and Chandrasekharan (34) proposed a water structure from x-ray diffraction experiments. This structure is characteristic of a "crystalline" water fraction with multiple bonding, but ignores the dynamical properties of molecules. Indeed, the only information available comes from the oxygen of water molecules because the hydrogens are so small. In this molecular structure, the water molecules are immobilized on two possible sites of the helix by forming two types of linkages between neighboring chains (NH—O_wH—O=C, C=O—H–O_w—H—O=C, where O_w is an oxygen from a water molecule). In this specific binding model, the sites must be defined more precisely in order to explain the NMR measurements and the orientation effects.

In a model where the tropocollagens are treated as cylindrically symmetrical systems, Berendsen and Migchelsen (22, 23) made a theoretical calculation of the second moment $S(\alpha, \theta)$ of the spectral lines for collagen as a function of two angles, α between the fiber and the direction of the proton interaction, and θ between the fiber and the field. Comparing the width of the experimental lines with the calculated second moment, Berendsen obtained a good agreement when the direction of the proton interaction was close to the fiber direction ($\alpha < 15°$). Hence, he suggested that water molecules form chains in the fiber direction and that these chains rotate and reorient about their own axes. This mechanism of chain rotation induces the resulting proton interaction to lie along or close to the fiber axis. However, the amino-acid sequences of natural tropocollagen are much less regular than the structure schematized by Berendsen and does not present the periodicity needed by the building of simple water chains. Nevertheless, our results confirm the idea of an effective interaction direction close to the fiber axis, as introduced by Berendsen.

If the vector connecting the two protons on a water molecule is along the magnetic field, the dipolar splitting in the spectra is 21 G. This maximum value is not observed, and Migchelsen and Berendsen (23) expressed the reduction factor of the splitting in terms of three S parameters which describe the average orientation of a molecule with respect to the macroscopic collagen symmetry axis. Calculated for the two-site structure of Ramachandran, the most appropriate parameters were found to correspond to a preferential orientation of water molecules with their H—H direction perpendicular to the fiber axis ($\alpha = 90°$); this is inconsistent with the chain model. Using the S parameters in the analysis of the NMR line splitting, Grigera et al. (36) determined two angles, $\alpha = 42°$ and $\alpha = 90°$, for the two sites of Ramachandran. The T_2 values were also derived from the line width at the 0° and 90° orientations of the fiber, and the ratio $T_2(0°)/T_2(90°) = 1.2$ was compared with the theoretical value obtained with the S parameters deduced from the line splitting. A good agreement was found, but this contradicts our results which clearly show that the shortest relaxation time appears when the fiber is aligned along the magnetic field. Furthermore, dielectric measurements (36) and water adsorption data (35) performed by Grigera and Berendsen demonstrate that two types of bound water molecules exist: one type strongly bound to the macromolecules in the two different sites and another type only weakly influenced by the macromolecules. These types of water molecules naturally refer to the water fractions that we have called interstitial and hydration fractions in the present description.

The study of collagen spectra gives a global picture of the relaxation behavior, whereas the deconvolution of the transverse decay curves allows the detailed examination of the interstitial water by isolating the different contributions. Indeed, the doublet of lines in the collagen spectra arises from three different water fractions and includes the effects of cross-relaxation coupling with macromolecules.

Let us reconcile the previous descriptions of the interstitial water with the well-known model of Woessner and Zimmerman, (44, 45) adding the dynamical details of the water molecules' motion. Water molecules are enclosed into the triple helix and are fixed by two hydrogen bonds according to the hydration model of Ramachandran. Water molecules can rotate about the axis defined by the two bonds. The reorientation of this rapid rotation axis occurs when hydrogen bonds break and reform other ones in the complex macromolecular structure. When reorienting, the axis must remain in a plane determined by the possible bonds in a site; this plane is thus parallel to the fiber axis. We can describe the motions in the following coordinate system: the rotating proton–proton vector

makes an angle δ with the rotation axis so that the direction of the interaction moves on a cone. Let α be the angle between the rotation axis and H_0, the static field. In the high field approximation and assuming two possible values for δ (0°–38°) and a very short rotation correlation time ($\omega\tau_c \ll 1$), the expression for T_2 given by Woessner is reduced to:

$$\frac{1}{T_2} = \frac{9}{128}\gamma^4\hbar^2 r^{-6} < (3\cos^2\delta - 1)^2(1 - 3\cos^2\alpha)^2 > \tau_M, \quad (14)$$

where r is the interproton distance and τ_M is the correlation time for axis reorientation, i.e., for simultaneous change of δ and α.

For the explicit calculation of Eq. 14 to be performed, the angular probability distribution function must be specified. It is obvious that this function depends on θ, the fiber-to-field angle. Moreover, the dependence of $1/T_2$ on $(1 - 3\cos^2\theta)^2$ must be reproduced. This feature can be checked by testing two different assumptions corresponding, respectively, to a fast and a slow reorientation process. In the first case we use a Gaussian probability density centered about $\alpha = \theta$, with standard deviation σ. In the second case, α is allowed to take two equally probable values $\theta + \theta_1$ and $\theta - \theta_1$, one for each binding mode on one site. Both cases lead to the same conclusion: $1/T_2$ is proportional to $(1 - 3\cos^2\theta)^2$ only if $\sigma = 0$ or $\theta_1 = 0$, respectively. We are thus led to a model where the rotation axes are essentially aligned along the fiber axis. As a result of the rapid rotation, the details of the motion disappear and the effective proton–proton interaction occurs along this rotation axis.

Moreover, the factor containing δ in Eq. 14 indicates that the contribution of $\delta = 0°$ dominates $\delta = 38°$ (4 against 0.7). This binding mode corresponds to the case where the two hydrogens of a water molecule are linked to the macromolecule. This is the most favorable position for alignment along the fiber axis, since the distance between the binding points is larger than when water oxygen is involved.

Finally, the values of τ_M are estimated from the T_2 of Table 3, using $r = 1.5$ Å: τ_M varies from 10^{-8} to 6×10^{-9} s between 10°C and 30°C. This correlation time τ_M depends on the lifetime of hydrogen bonds (τ_H) and on the axis reorientation correlation time (τ_R). Reorientation motion, as well as the hydrogen bond breaking and reforming, is thought to be a direct consequence of the rapid rotation. The global reorientation mechanism in which a water molecule changes its binding mode is governed by the rapid rotational motion, because all the processes are intimately correlated. τ_R and τ_H are thus of the same order and it is difficult to determine them separately. The values of the correlation times τ_R are quite consistent with the values established, for example, for lysozyme solutions (46), and τ_H corresponds to the recently estimated lifetime of a hydrogen bonded water molecule (33).

Returning to the previous discussion about K_a, it appears that the magnetization transfer is partially induced by the same fast dynamics. Consequently, the extreme narrowing condition must be applied to have K_a proportional to τ_{CR}. The time scale of the motions of functional groups on macromolecules is probably of the same order and thus $\omega\tau_{CR} \ll 1$. The values of the intrinsic relaxation times calculated in Table 3 may appear unexpected: T_2 for functional groups is ~1 ms, which is long compared with usual relaxation times in solids and shorter than the values for water protons, even in the most tightly bound fraction. Our interpretation is that the interactions among macromolecular protons along the fiber axis remain the dominant anisotropic relaxation mechanism, that the functional groups are much more mobile than nuclei imbedded inside the macromolecule (they are essentially as mobile as the water molecules that interact with them), but that their relaxation rate is enhanced compared with water relaxation by spin diffusion toward the very fast relaxing protons of the glycines. For this reason, the protons of the functional groups have a T_2 shorter than the protons of the interstitial water.

The dynamical characteristics of collagen have now been made clearer: the image of the fiber that results from our measurements is less static than the one previously derived from x-ray diffraction. The correlation time of the motion of the interstitial water, translation and rotation being intimately involved in the same process of axis reorientation, is of the same order of magnitude as the lifetime of a H-bond ($\approx 10^{-9}$ s). The protons of the interstitial water interact with each other along an effective mean direction parallel to the axis of the fiber. This statement, already made by Berendsen in his early study of collagen (21), has now been clarified by the values of T_2 obtained for a fiber orthogonal to the field and for a fiber aligned on it, owing to the four-component deconvolution of the spin-echo amplitude decay.

We are grateful to Dr. Robert Muller for his constant interest in our work, and for his many suggestions for improving it. The help of Frederic Maton and Helmut Fisher in performing the relaxation measurements was highly appreciated. We thank Drs. Seymour H. Koenig and Rodney D. Brown III for our first tendon dispersions, which were recorded in their laboratory (IBM T.J. Watson Research Center, Yorktown Heights, N.Y.).

Received for publication 25 April 1988 and in final form 26 May 1989

REFERENCES

1. Koenig, S. H., and R. D. Brown. 1987. *Relaxometry of tissue. In* NMR Spectroscopy of Cells and Organisms. R. K. Gupta, editor. CRC Press, Boca Raton, FL. 2:75–114.

2. Cooke, R., and R. Wien. 1971. The state of water in muscle tissue as determined by proton nuclear magnetic resonance. *Biophys. J.* 11:1002–1017.
3. Hazlewood, C. F., B. L. Nichols, and N. F. Chamberlain. 1969. Evidence for the existence of a minimum of two phases of ordered water in skeletal muscle. *Nature (Lond.)* 222:747–750.
4. Fung, B. M. 1977. Correlation of relaxation time with water content in muscle and brain tissue. *Biochim. Biophys. Acta.* 497:317–322.
5. Hazlewood, C. F., D. C. Chang, B. L. Nichols, and D. E. Woessner. 1974. Nuclear magnetic resonance transverse relaxation times of water protons in skeletal muscle. *Biophys. J.* 14:583–606.
6. Zimmerman, J. R., and W. E. Brittin. 1957. Nuclear magnetic resonance studies in multiple phase systems: lifetime of a water molecule in an adsorbing phase on silica gel. *J. Phys. Chem.* 61:1328–1333.
7. Resing, H. A., A. N. Garroway, and K. R. Foster. 1976. Bounds on bound water: transverse and rotating frame NMR relaxation in muscle tissue. *Magn. Reson. Colloid. Interface Sci., ACS Symp.* 34:516–529.
8. Resing, H. A. 1976. Quadrupole coupling constants in adsorbed water. Effects of chemical exchange. *J. Phys. Chem.* 80:186–193.
9. Luz, Z., and S. Meiboom. 1963. Nuclear magnetic resonance study of the protolysis of trimethylammonium ion in aqueous solution: order of the reaction with respect to solvent. *J. Chem. Phys.* 39:366–370.
10. Gutowsky, H. S., R. L. Vold, and E. J. Wells. 1965. Theory of chemical exchange effects in magnetic resonance. *J. Chem. Phys.* 43:4107–4125.
11. Allerhand, A., and H. S. Gutowsky. 1964. Spin-echo NMR studies of chemical exchange. I. Some general aspects. *J. Chem. Phys.* 41:2115–2126.
12. Allerhand, A., and H. S. Gutowsky. 1965. Spin-echo studies of chemical exchange. II. Closed formulas for two sites. *J. Chem. Phys.* 42:1587–1599.
13. Fung, B. M. 1986. Nuclear magnetic resonance study of water interactions with proteins, biomolecules, membranes, and tissues. *Methods Enzymol.* 127:151–161.
14. Fung, B. M., and P. S. Puon. 1981. Nuclear magnetic resonance transverse relaxation in muscle water. *Biophys. J.* 33:27–37.
15. Koenig, S. H., R. G. Bryant, K. Hallenga, and G. S. Jacob. 1978. Magnetic cross-relaxation among protons in protein solutions. *Biochemistry.* 17:4348–4358.
16. Escanye, J. M., D. Canet, and J. Robert. 1984. Nuclear magnetic relaxation studies of water in frozen biological tissues. Cross-relaxation effects between protein and bound water protons. *J. Magn. Reson.* 58:118–131.
17. Edzes, H. T., and E. T. Samulski. 1977. Cross relaxation and spin diffusion in the proton NMR of hydrated collagen. *Nature (Lond.)* 265:521–523.

17*a*. Edzes, H. T., and E. T. Samulski. 1978. The measurement of cross-relaxation effects in the proton NMR spin-lattice relaxation of water in biological systems: hydrated collagen and muscle. *J. Magn. Reson.* 31:207–229.

18. Fung, B. M., and T. W. McGaughy. 1980. Cross relaxation in hydrated collagen. *J. Magn. Reson.* 39:413–420.
19. Renou, J. P., J. Alizon, M. Dohri, and H. Robert. 1983. Study of the water-collagen system by NMR cross relaxation experiments. *J. Biochem. Biophys. Methods.* 7:91–99.
20. Wise, W. B., and P. E. Pfeffer. 1987. Measurement of cross-relaxation effects in the proton NMR of water in fibrous collagen and insoluble elastin. *Macromolecules.* 20:1550–1554.
21. Berendsen, H. J. C. 1962. Nuclear magnetic resonance study of collagen hydration. *J. Chem. Phys.* 36:3297–3305.
22. Berendsen, H. J. C., and C. Migchelsen. 1965. Hydration structure of fibrous macromolecules. *Ann. NY Acad. Sci.* 125:365–379.
23. Migchelsen, C., and H. J. C. Berendsen. 1973. Proton exchange and molecular orientation of water in hydrated collagen fibers. An NMR study of H_2O and D_2O. *J. Chem. Phys.* 59:296–305.
24. Dehl, R. E., and C. A. J. Hoeve. 1969. Broad-line NMR study of H_2O and D_2O in collagen fibers. *J. Chem. Phys.* 50:3245–3251.
25. Dehl, R. E. 1970. Collagen: mobile water content of frozen fibers. *Science (Wash. DC).* 170:738–739.
26. Cleveland, G. G., D. C. Chang, C. F. Hazlewood, and H. E. Rorschach. 1976. Nuclear magnetic resonance measurement of skeletal muscle. *Biophys. J.* 16:1043–1053.
27. Kasturi, S. R., D. C. Chang, and C. F. Hazlewood. 1980. Study of anisotropy in nuclear magnetic resonance relaxation times of water protons in skeletal muscle. *Biophys. J.* 30:369–381.
28. Fullerton, G. D., I. L. Cameron, and V. A. Ord. 1985. Orientation of tendons in the magnetic field and its effect on T2 relaxation times. *Radiology.* 155:433–435.
29. Solomon, I. 1955. Relaxation processes in a system of two spins. *Physiol. Rev.* 99:559–565.
30. Andree, P. J. 1978. The effect of cross relaxation on the longitudinal relaxation times of small ligands binding to macromolecules. *J. Magn. Reson.* 29:419–431.
31. Winter, F., and R. Kimmich. 1985. $^{14}N^1H$ and $^2H^1H$ cross-relaxation in hydrated proteins. *Biophys. J.* 48:331–335.
32. Kimmich, R., F. Winter, and K.-H. Spohn. 1986. Interactions and fluctuations deduced from proton field-cycling relaxation spectroscopy of polypeptides, DNA, muscles, and algae. *J. Magn. Reson.* 68:263–282.
33. Koenig, S. H. 1988. Theory of relaxation of mobile water protons induced by protein NH moieties, with application to rat heart muscle and calf lens homogenates. *Biophys. J.* 53:91–96.
34. Ramachandran, G. N., and R. Chandrasekharan. 1968. Interchain hydrogen bonds via bound water molecules in the collagen triple helix. *Biopolymers.* 6:1649–1658.
35. Grigera, J. R., and H. J. C. Berendsen. 1979. The molecular details of collagen hydration. *Biopolymers.* 18:47–57.
36. Grigera, J. R., F. Vericat, K. Hallenga, and H. J. C. Berendsen. 1979. Dielectric properties of hydrated collagen. *Biopolymers.* 18:35–45.
37. Hoeve, C. A. J., and S. R. Kakivaya. 1976. On the structure of water absorbed in collagen. *J. Phys. Chem.* 80:745–749.
38. Hoeve, C. A. J., and A. S. Tata. 1978. The structure of water absorbed in collagen. *J. Phys. Chem.* 82:1660–1663.
39. Santyr, G. E., R. M. Henkelman, and M. J. Bronskill. 1988. Variation in measured transverse relaxation in tissue resulting from spin-locking with the CPMG sequence. *J. Magn. Reson.* 79:28–44.
40. Gillis, P., and B. Borcard. 1988. Nuclear magnetic relaxation dispersion of silica particle suspensions. *J. Magn. Reson.* 77:19–32.
41. Abragam, A. 1962. The Principles of Nuclear Magnetism. Oxford University Press, Oxford. 264–353.
42. Slichter, C. P. 1978. Principles of Magnetic Resonance. Springer-Verlag, Berlin. 56–76.

43. Lenk, R. 1986. Fluctuations, Diffusion and Spin Relaxation. Elsevier, Amsterdam. 216–230.

44. Woessner, D. E. 1962. Spin relaxation processes in a two-proton system undergoing anisotropic reorientation. *J. Chem. Phys.* 36:1–4.

45. Woessner, D. E., and J. R. Zimmerman. 1963. Nuclear transfer and anisotropic motional spin phenomena: relaxation time temperature dependence studies of water adsorbed on silica gel. IV. *J. Phys. Chem.* 67:1590–1600.

46. Fullerton, G. D., V. A. Ord, and I. L. Cameron. 1986. An evaluation of the hydration of lysozyme by an NMR tritration method. *Biochem. Biophys. Acta.* 869:230–246.